Archival Report

Biological Psychiatry: CNNI

Elevated Brain Iron in Cocaine Use Disorder as Indexed by Magnetic Field Correlation Imaging

Vitria Adisetiyo, Corinne E. McGill, William H. DeVries, Jens H. Jensen, Colleen A. Hanlon, and Joseph A. Helpern

ABSTRACT

BACKGROUND: Iron homeostasis is a critical biological process that may be disrupted in cocaine use disorder (CUD). In the brain, iron is required for neural processes involved in addiction and can be lethal to cells if unbound, especially in excess. Moreover, recent studies have implicated elevated brain iron in conditions of prolonged psychostimulant exposure. Thus, the purpose of this study was to examine iron in basal ganglia reward regions of individuals with CUD using an advanced imaging method called magnetic field correlation (MFC) imaging.

METHODS: MFC imaging was acquired in 19 non-treatment-seeking individuals with CUD and 19 healthy control individuals (both male and female). Region-of-interest analyses for MFC group differences and within-group correlations with age and years of cocaine use were conducted in the globus pallidus internal segment (GPi), globus pallidus external segment, putamen, caudate nucleus, thalamus, and red nucleus.

RESULTS: Individuals with CUD had significantly elevated MFC compared with control individuals within the GPi. In control individuals, MFC significantly increased with age in the GPi, globus pallidus external segment, putamen, and caudate nucleus. Conversely, there were no significant MFC within-group correlations in the CUD group.

CONCLUSIONS: Individuals with CUD have excess iron in the GPi, as indexed by MFC, and lack the age-related gradual iron deposition seen in normal aging. Because the globus pallidus is critical for the transition of goal-directed behavior to compulsive behavior, significantly elevated iron in the GPi may contribute to the persistence of CUD. These findings implicate dysregulation of brain iron homeostasis in CUD and support pursuing this new line of research.

Keywords: Addiction, Brain iron, Cocaine use disorder, Ferroptosis, Magnetic field correlation imaging, Psychostimulants

https://doi.org/10.1016/j.bpsc.2018.11.006

Psychostimulant dependence is an intransigent health problem that affects more than 1 billion individuals worldwide (1). Although psychostimulants comprise both legal substances (e.g., prescription amphetamine/methylphenidate, nicotine) and illegal substances (e.g., cocaine, methamphetamine), most exert their effects similarly through manipulations of monoamine neurotransmission (e.g., increase extracellular dopamine by blocking dopamine transporters at striatal terminals) (2). Cocaine is the most widely used illicit psychostimulant in the United States, with nearly 1 million Americans meeting criteria for cocaine use disorder (CUD) (3). Chronic cocaine use has been associated with downregulation of the striatal dopaminergic system (4) and aberrant resting-state and cue-evoked blood oxygen level–dependent signals in cortico-striatal networks (5,6). As such, CUD is predominantly regarded as a disease of the brain's dopaminergic reward system (7). Despite more than 2 decades of research, however, CUD and methamphetamine use disorder are the only substance use disorders without an effective pharmacotherapy (8,9). The neurobiological mechanisms driving maladaptive changes in CUD are not fully understood and may explain why effective medication treatments remain elusive (9). One potential mechanism, and the guiding hypothesis of this study, is that the intransigence of CUD may be exacerbated by the confounding effects that chronic cocaine use has on brain iron homeostasis in the basal ganglia—the stimulus–response interface of the brain's reward circuit (10,11).

Iron homeostasis is a critical biological mechanism that has been underexamined in addiction (12–19). Iron is required for virtually all basic cellular processes, and it transitions between two oxidation states for its diverse functions, ferric iron and ferrous iron (20). Most circulating iron is in the protein-bound ferric iron form because free iron is lethal to cells, especially in large concentrations (21). Specifically, free iron acts as a catalyst in the formation of harmful free radicals from reactive oxygen species via the Fenton reaction (21,22). Accordingly, intricate regulatory mechanisms that control iron uptake and redistribution processes exist on the systemic and cellular levels to safely sequester iron in a bound form while ensuring that the iron supply meets the body's vast demands (23,24).

Under physiological conditions, the rate of iron movement across the blood-brain barrier (BBB) into the brain is tightly controlled and depends on the brain's iron status and biological needs (25–28).

Brain iron is required for neural processes implicated in addiction, including dopamine synthesis and regulation, myelin metabolism, and blood oxygen transport (29–31). As such, maintaining iron homeostasis not only is essential for healthy brain development and aging but also likely affects the behavioral actions of psychostimulants. For example, low brain iron impairs dopamine and myelin metabolism (32–35) and has been associated with developmental delay (36,37), whereas excess iron causes an iron-dependent form of cell death called ferroptosis that is prevalent in neurodegenerative diseases (24,38,39). Moreover, animal studies of iron deficiency found that reduced dopamine transporters and receptors in the striatum and ventral striatum (12–14) attenuate the effects of cocaine (15,17). Conversely, mechanisms that promote brain iron accumulation, including chronic inflammation (40–45) and increased BBB permeability (46,47), have been detected in CUD, suggesting that iron dysregulation is likely present in cocaine addiction. These observations are in concordance with recent studies that implicate elevated brain iron within basal ganglia regions in conditions of prolonged psychostimulant exposure, including prescription amphetamine/methylphenidate in attention-deficit/hyperactivity disorder and methamphetamines in vervet monkeys (16,19,48).

As an extension of this prior research, the purpose of this study was to examine brain iron in the basal ganglia of individuals with CUD, focusing on regions implicated in the transition of goal-directed behavior to compulsive behavior (49,50). While proton transverse relaxation rates are conventionally used to quantify brain iron with magnetic resonance imaging (MRI), they have limited specificity for iron (51). Therefore, we used an advanced method called magnetic field correlation (MFC) imaging (52–54), which quantifies intravoxel magnetic field inhomogeneities (MFIs) generated by tissue iron. MFC is independent of dipolar relaxation mechanisms, thereby improving its specificity for iron (54). The predominant forms of brain iron are ferritin and hemosiderin iron (55), and these are distributed in a complex spatial pattern both macroscopically (56) and microscopically (57–59). In the applied field of an MRI scanner, ferritin and hemosiderin iron, which are strongly magnetic (60,61), generate a complex pattern of MFIs down to cellular length scales. The MFC is thus a tissue property characterizing the microscopic (i.e., intravoxel) distribution of storage iron. Another iron-related physical property that is independent of dipolar relaxation mechanisms is the magnetic susceptibility, which can be assessed on a macroscopic (i.e., intervoxel) level with quantitative susceptibility mapping (QSM) (62,63). As a consequence, MFC and QSM provide distinct but complementary information, and both may be reasonably regarded as relative indices of brain iron, particularly in deep gray matter regions (54,62–64).

Given that the striatum (i.e., putamen [PUT] and caudate nucleus [CN]) is the primary target of cocaine, and that the globus pallidus internal segment (GPi) and globus pallidus external segment (GPe) are the dual output pathways of the striatum (49,65), we hypothesized that individuals with CUD will have excess iron levels (as indexed by elevated MFC) within these key reward regions of the basal ganglia. While there exists one prior study of brain iron in CUD using QSM (19), this is the first MFC imaging study of CUD.

METHODS AND MATERIALS

Participants

A total of 25 non-treatment-seeking cocaine users were recruited from the community. Of these individuals, 6 were excluded owing to severe motion artifacts in their neuroimaging data. All remaining 19 individuals (79% male) met the DSM-IV-TR criteria for cocaine dependence and had a positive urine drug screen for cocaine at the time of assessment (Multi-Drug Screen Test Dip Card; W.H.P.M. Inc., Irwindale, CA). A total of 19 age-matched healthy control individuals (58% male) without a history of drug, nicotine, or alcohol abuse/dependence were also recruited from the community (66). A review of medical history was conducted for all participants. Diagnosis of CUD and other psychiatric disorders was determined by the Mini-International Neuropsychiatric Interview for DSM-IV (67). The Fagerström Test for Nicotine Dependence (68,69), Beck Depression Inventory (70), and Alcohol Use Disorders Identification Test (71) were also administered. For the CUD group, inclusion required a primary diagnosis of cocaine dependency.

Exclusion criteria consisted of major medical or neurological illness, lifetime history of a psychotic disorder, history of a traumatic head injury, and contraindications to MRI. For the CUD group, individuals were excluded if they met criteria for a personality disorder or current mood disorder. For control individuals, a history of DSM-IV-TR diagnoses and reports of iron deficiency were exclusionary. The study was approved by the Medical University of South Carolina's Institutional Review Board, and written informed consent was obtained from all participants. Four participants were taking regular medication: one participant with CUD on citalopram for mild depression, one participant with CUD on tramadol for headaches, one control participant on omeprazole for gastroesophageal reflux disease, and one control participant on meloxicam for rheumatoid arthritis. Participants were instructed to not take any medication or drugs on the scan day. Because all the individuals with CUD were actively abusing cocaine, they were further instructed not to use any substances the day before the MRI visit. On the scan day, drug abstinence for methamphetamine, cocaine, opiates, and benzodiazepines was verified by negative urine drug screen results; one participant with CUD had a positive urine drug screen for tetrahydrocannabinol. Cohort demographics are summarized in Table 1.

Image Acquisition and Processing

Participants underwent an MRI brain scan using a 3T Siemens TIM Trio scanner (Siemens, Erlangen, Germany). Whole-brain structural T1-weighted magnetization prepared rapid acquisition gradient-echo images were acquired with the following parameters: repetition time = 1900 ms, echo time = 2.34 ms, voxel size = $0.9 \times 0.9 \times 1.0$ mm^3, field of view = 220 mm^2, slices = 192, flip angle = 9°, acquisition time = 5 minutes 42 seconds. For MFC estimation, asymmetric spin-echo (ASE) images were acquired with the segmented echo-planar imaging approach, which minimizes echo-planar imaging distortion (72):

Table 1. Demographics

	Control Group (n = 19)	CUD Group (n = 19)	Group Comparison	
			t	p Value
Age, Years, Mean ± SD	36.9 ± 12.5	41.0 ± 9.2	1.16	.252
Age Range, Years	19.2–59.6	21.4–54.6	–	–
Gender, Male:Female, n	15:4	11:8	Fisher's	.295
Current Primary Diagnosis: CUD, n	0	19	–	–
Years of Cocaine Use, Mean ± SD	0	19.6 ± 9.4	–	–
Years of Cocaine Use, Range	0	3–36	–	–
Age First Used Cocaine, Years, Mean ± SD	0	20.8 ± 5.2	–	–
Age Range First Used Cocaine, Years	0	14–35	–	–
Days Since Last Used Cocaine, Mean ± SD	0	2.6 ± 1.1	–	–
Days Since Last Used Cocaine, Range	0	1–4	–	–
Days Used Cocaine/Last 30 Days, Mean ± SD	0	10.8 ± 6.1	–	–
Days Used Cocaine/Last 30 Days, Range	0	1–25	–	–
Type: Powdered Cocaine, n	0	10	–	–
Type: Crack Cocaine, n	0	6	–	–
Type: Powdered Cocaine + Crack Cocaine, n	0	3	–	–

CUD, cocaine use disorder (dependence, non-treatment-seeking); –, not applicable; t, Student's t test.

repetition time = 5550 ms, echo time = 40 ms, voxel size = 1.7 × 1.7 × 1.7 mm^3, field of view = 220 mm^2, slices = 40, flip angle = 90°, bandwidth = 1346 Hz/pixel, echo-planar imaging factor = 33, refocusing pulse time shifts = 0, −4, and −16 ms, no gaps, average = 4, acquisition time = 6 minutes 40 seconds. Prior to MFC calculation, the ASE images were corrected for Gibbs-ringing artifacts (73) and were motion corrected (see Supplement). The MFC parametric map was then calculated on a voxel-by-voxel basis (52,53). Structural scans were screened by two experienced raters (WHD and VA) for gross abnormalities and referred to a neuroradiologist when warranted. Images with incidental findings of clinical significance or severe artifacts (e.g., blurred images, signal loss) were excluded.

Region-of-Interest Analyses

Region-of-interest (ROI) analyses were conducted on the GPe, GPi, PUT, CN, and red nucleus (RN) because these brain regions have the highest concentrations of dopamine and iron (29,56), are targets of cocaine (74), are implicated in the transition of goal-directed behavior to compulsive behavior (49,50), and have been previously studied in CUD (19). The thalamus (THL) was also examined as a control ROI. To optimize anatomical accuracy, automated ROI segmentation was conducted on each participant's high-resolution magnetization prepared rapid acquisition gradient-echo using the FreeSurfer software (http://surfer.nmr.mgh.harvard.edu). Every participant's ROIs, 0-shift ASE image, and MFC map were then normalized (resliced and resampled) to the Montreal Neurological Institute 152 standard space (1 mm^3) using the nonlinear registration algorithm from the Automatic Registration Toolbox software (75).

The whole GP ROI was manually delineated into the GPe and GPi by tracing the dividing boundary on each participant's normalized 0-shift ASE image. To exclude voxels with partial volume effects, ROIs were further constrained with a consensus mask. The PUT, CN, and THL consensus masks were defined as ROI voxels with 100% overlap among all participants; given the smaller structures of the GPe and GPi, their consensus masks were defined by a minimum of 79% overlap (30 of 38, the most conservative threshold that preserved anatomy). Owing to the unavailability of automatic RN segmentation, the RN consensus ROI was drawn on a normalized group average 0-shift ASE image with its boundary defined well within the clearly distinguishable anatomical boundary to avoid partial volume effects. For each participant, anatomical accuracy of the consensus ROIs was visually verified (Figure 1A) and applied to the normalized MFC map to extract ROI means.

Statistical Analyses

Statistical analyses were performed with SPSS software (version 24.0; IBM Corp., Armonk, NY). Data distributions were tested for normality with the Shapiro-Wilk test. Group comparisons were conducted using the two-tailed Student's t test for normally distributed measures (Cohen's d for effect size), the Mann-Whitney U test for non-normally distributed measures (rank biserial correlation for effect size), and the Fisher's exact test for nominal measures. A sequential Bonferroni-type false discovery rate (FDR) correction method was conducted to correct for multiple comparisons where an FDR corrected p value significance threshold is calculated (76). The FDR approach was applied over the entire set of p values from each type of analysis (e.g., between-group comparison). ROI MFC within-group correlations with age and collinearity tests were conducted using Pearson's correlation for normally distributed measures and Spearman's correlation for non-normally distributed measures, all two-tailed. In the CUD group, correlations of MFC with age of first cocaine use, timing of cocaine use, and MFC partial correlations with years of cocaine use (controlling for age) were conducted for each ROI.

RESULTS

Demographics and MFC Index of Brain Iron

The two groups did not significantly differ in age or gender ratio (Table 1). The CUD group had a moderate level of

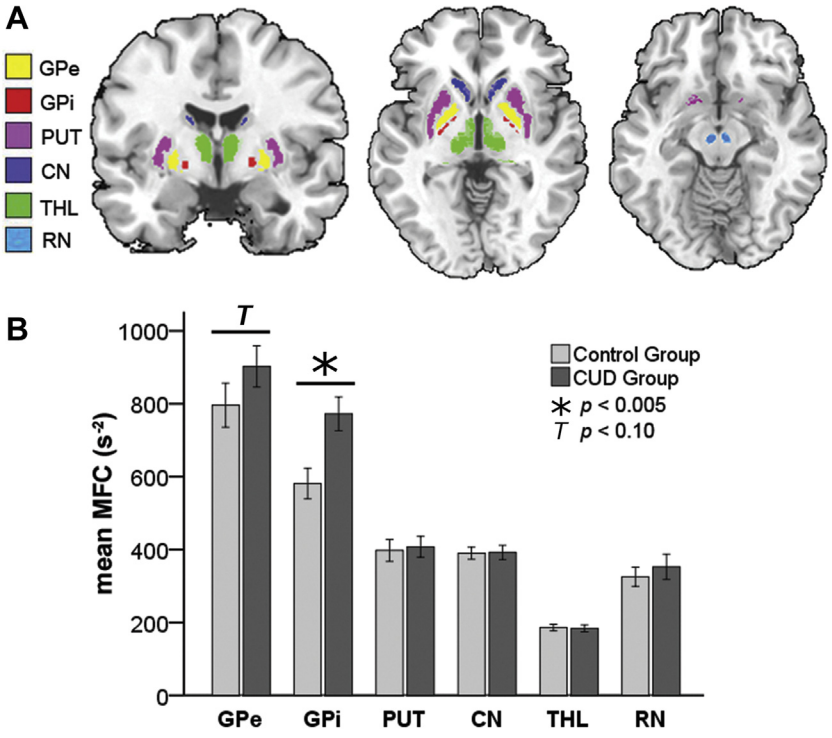

Figure 1. Group differences in magnetic field correlation (MFC) indices of brain iron between control individuals and individuals with cocaine use disorder (CUD). **(A)** Region-of-interest analyses were conducted on the globus pallidus external segment (GPe), globus pallidus internal segment (GPi), putamen (PUT), caudate nucleus (CN), thalamus (THL), and red nucleus (RN). **(B)** The CUD group had significantly higher MFC values than the control group in the GPi (rank biserial correlation = .50, survived false discovery rate correction) and had a similar trend in the GPe (rank biserial correlation = .30). There were no significant group differences or trends in the PUT, CN, THL, or RN. Standard errors are shown.

depressive symptoms (Beck Depression Inventory score: mean = 11.1, SD = 9.9). In the CUD group, 3 individuals had a history of posttraumatic stress disorder, 3 individuals had a previous episode of major depressive disorder (2 of them with a suicide attempt), 1 individual had a history of panic disorder, and 1 individual met criteria for generalized anxiety disorder. In the CUD group, 16 individuals were regular nicotine smokers (Fagerström score: mean = 2.9, SD = 2.3), 4 individuals met criteria for alcohol use disorder (Alcohol Use Disorders Identification Test score: mean = 10.1, SD = 6.5), and 5 individuals reported marijuana use at least one time per week.

The CUD group had significantly higher MFC values in the GPi (median = 778 s^{-2}, range = 484–1049 s^{-2}) than the control group (median = 559 s^{-2}, range = 386–1148 s^{-2}). This significant difference has a large effect size (rank biserial correlation = .50) and survived FDR correction. There was also a similar trend in the GPe (CUD group: median = 923 s^{-2}, range = 475–1357 s^{-2}; control individuals: median = 705 s^{-2}, range = 547–1495 s^{-2}) with a medium effect size (rank biserial correlation = .30), but this group difference did not meet statistical significance ($p < .10$). There were no significant group differences or trends in the PUT, CN, THL, and RN (Table 2 and Figure 1B). These findings were replicated when age was controlled as a covariate (Supplemental Table S2).

MFC as a Function of Age and Cocaine Use

In the control group, MFC values significantly increased with age in the GPe, GPi, PUT, and CN, with a similar trend in the RN; there was no age correlation in the THL. In the CUD group,

Table 2. MFC Group Comparisons

			Group Comparison			
MFC (s^{-2})	Control Group (n = 19), Mean (SD)	CUD Group (n = 19), Mean (SD)	CUD % Difference	Statistic	p Value	Effect Size
GPe	796 (264)	903 (246)	+13.4	U = 123	.096	r_{rb} = .30; Medium
GPi	581 (183)	772 (202)	+32.9	U = 82	.003[a]	r_{rb} = .50; Large
PUT	398 (131)	408 (125)	+2.4	t = −0.23	.819	d = .10; Small
CN	390 (72)	392 (86)	+0.5	t = −0.08	.935	d = .00; Small
THL	186 (40)	184 (41)	−1.2	t = 0.17	.864	d = .10; Small
RN	325 (115)	353 (151)	+8.5	t = −0.63	.532	d = .20; Small

CN, caudate nucleus; CUD, cocaine use disorder; d, Cohen's d; GPe, globus pallidus external segment; GPi, globus pallidus internal segment; MFC, magnetic field correlation; PUT, putamen; RN, red nucleus; r_{rb}, rank biserial correlation; t, Student's t-test; THL, thalamus; U, Mann-Whitney U test, exact significance.

[a]Survived false discovery rate correction.

MFC values did not correlate with age in any of the ROIs (Table 3 [top] and Figure 2) or with years of cocaine use, even when controlling for age (Table 3, bottom) or vice versa ($p > .05$) (not shown). MFC values also did not correlate with the age that the individual with CUD first used cocaine in any of the ROIs (Table 3, bottom) or with the timing of cocaine use (i.e., days since last used cocaine and days used cocaine in last 30 days; $p > .05$) (not shown). All significant findings survived FDR correction.

DISCUSSION

Brain iron homeostasis is a critical biological mechanism that has been underexamined in CUD, with only one prior study to date (19). Using MFC imaging to index brain iron, we demonstrated that individuals with CUD have significantly elevated MFC values in the GPi (32.9% increase) compared with control individuals, with a similar trend in the GPe (13.4% increase). Moreover, unlike in control individuals, there were no significant correlations of MFC with age in the CUD group within the GPi, GPe, PUT, and CN. These MFC data corroborate previous QSM findings in CUD by Ersche *et al.* (19) and are consistent with preclinical work in animals that demonstrates altered cocaine response with iron dysregulation (12–15,17); detection of similar aberrant findings using two different advanced iron MRI methods in two separate cohorts provides strong concordant evidence of disrupted brain iron homeostasis in cocaine addiction. Our findings also add to the literature that supports elevated brain iron levels in conditions of prolonged psychostimulant exposure (16,48).

Table 3. MFC Within-Group Correlation Analyses

Correlations With Age		
MFC (s^{-2})	Control Group (n = 19), r (p Value)	CUD Group (n = 19), r (p Value)
GPe	r_s = .77 (<.001)[a]	−.19 (.444)
GPi	r_s = .50 (.029)[a]	−.09 (.713)
PUT	.72 (<.001)[a]	−.23 (.342)
CN	.60 (.006)[a]	−.11 (.662)
THL	.36 (.134)	.21 (.378)
RN	.40 (.092)	.30 (.213)

Correlations With Years of Cocaine Use and Age at First Use of Cocaine			
	CUD Group (n = 19)		
MFC (s^{-2})	Years of Cocaine Use, r (p Value)	Years of Cocaine Use (Controlling for Age),[b] r (p Value)	Age at First Use of Cocaine, r_s (p Value)
GPe	−.10 (.688)	.11 (.663)	−.26 (.286)
GPi	−.10 (.673)	−.05 (.840)	.06 (.797)
PUT	−.09 (.706)	.19 (.442)	−.33 (.168)
CN	−.12 (.625)	−.06 (.828)	−.84 (.732)
THL	.06 (.806)	−.23 (.365)	.16 (.505)
RN	.43 (.066)	.35 (.159)	−.29 (.235)

CN, caudate nucleus; CUD, cocaine use disorder; GPe, globus pallidus external segment; GPi, globus pallidus internal segment; MFC, magnetic field correlation; PUT, putamen; r, Pearson's correlation; RN, red nucleus; r_s, Spearman's correlation; THL, thalamus.

[a]Survived false discovery rate correction.

[b]Partial correlations.

Elevated GP Iron in CUD

The consistency of our elevated MFC findings in the GP with previous QSM findings in CUD (19) and histology findings in methamphetamine-exposed monkeys (16) suggests that there may be regional specificity of elevated iron with psychostimulant abuse. While not evaluated in our study, chronic inflammation and increased BBB permeability have been documented in CUD (40–47,77) and are potential mechanisms promoting elevated GP iron. Inflammation increases BBB permeability and triggers aberrant molecular cascades that signal cells to sequester iron regardless of need (24,46,78). Genetic influences on iron status in CUD may also contribute to our findings. Studies of patients with inherited neurodegeneration with brain iron accumulation disorders have identified genetic mutations that alter iron-related regulatory proteins, providing insight into other potential mechanisms (79,80). Excess iron causes ferroptosis, characterized by chronic inflammation and cytosolic accumulation of free iron and lipid hydroperoxides (24,81,82). Although speculative, our findings suggest that there may be increased risk for neurodegeneration in the GPi. It is important to note that the majority of brain iron is stored as ferric iron in ferritin (55), and so it is this storage iron pool that likely generates the MFIs detected by MFC imaging. Nonetheless, ferritin iron is believed to be in equilibrium with free iron, and so MFC may indirectly reflect this iron pool as well (51,83,84). Indeed, there is postmortem evidence of neuronal death associated with chronic cocaine use in humans, including loss of dopamine neurons (77) and selective lesions in the GP (85–87).

Specific disruption of GP functioning, via neurodegeneration or other unknown iron-related mechanisms (79,80,88–90), may contribute to the persistence of CUD. As part of the dual output pathways of the striatum (65), the GPi and GPe are key regions involved in the transition of goal-directed behavior to compulsive behavior that is the hallmark of addiction (11,49,50,91–93). The GPi is part of the direct/go/prepare pathway associated with executing goal-directed behaviors (11,94,95) and receives input from executive control frontal areas via the CN (50). Alternatively, the GPe is part of the indirect/no-go/selection pathway associated with exploitation of habitual behavior (11,94,95). Because the interaction of these pathways determines the time course and activity profile of the output nuclei (96), functional disruption in either the GPi or GPe could bias behavior in one direction (97). Elevated GPi iron in CUD could reflect greater disruption in the direct/go/prepare pathway, reinforcing bias toward habitual behavior. This speculation is consistent with studies that demonstrate obsessive compulsive traits with GPi manipulations or lesions (88–90,98) and may coincide with the executive control dysfunction observed in CUD (99–101).

Comparable Striatal Iron in CUD and Control Individuals

Similar to previous QSM findings in CUD (19), there were no MFC group differences in the striatum, including the nucleus accumbens (Supplemental Table S1 and Supplemental Figure S1). This observation was surprising because the striatum is a primary target of psychostimulants (74). Given that the brain's physiological demands for iron are region

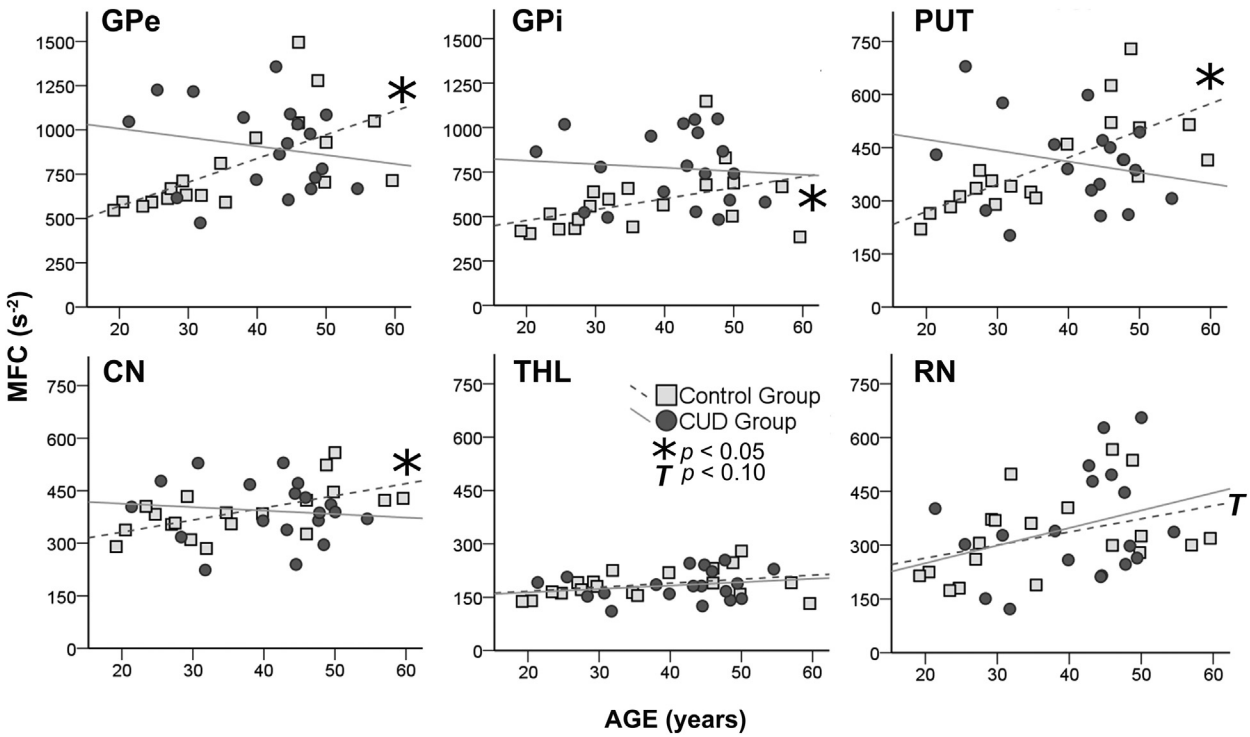

Figure 2. Magnetic field correlation (MFC) indices of brain iron correlate with age in control individuals but not in individuals with cocaine use disorder (CUD). In the control group, MFC indices of brain iron significantly increased with age in the globus pallidus external segment (GPe), globus pallidus internal segment (GPi), putamen (PUT), and caudate nucleus (CN) but not in the thalamus (THL) or red nucleus (RN); there was a trend in the RN. Conversely, in the CUD group, there were no significant correlations or trends of MFC with age in any of the aforementioned regions. All significant correlations survived false discovery rate correction.

dependent (29,56), vulnerability to iron dysregulation in pathology may also vary by region. For example, higher continuous firing rates of pallidal neurons compared with striatal neurons may differentially affect iron use (102). Indeed, the GP is known to have the highest physiological levels of brain iron (56,64,103) and requires specialized mechanisms to sequester high iron concentrations (104); these features may contribute to GP vulnerability to iron overload. In contrast, regulation of lower physiological iron levels in the PUT and CN (56,64,103) may be less sensitive to disruption. It is also possible that lower iron levels in the striatum may reduce the MFC's sensitivity to detect striatal iron. However, this effect would be minimal given that the sensitivity of MFC to index iron in the PUT and CN has been demonstrated in healthy individuals (64) and in individuals with attention-deficit/hyperactivity disorder (48). Alternatively, our negative cross-sectional findings could be masking dynamic changes occurring in CUD (105).

Gradual Accumulation of Brain Iron in Normal Aging Is Altered in CUD

Basal ganglia regions accumulate iron at different rates throughout normal development and aging (29,56), and they support various components of cognitive and motor functioning (106–108). Consistent with the well-documented increase of brain iron in healthy aging (56,64,103), MFC values significantly increased with age in control individuals within the GPe, GPi, PUT, and CN. The lack of age correlation in the THL aligns with postmortem studies of normal aging given that THL iron levels plateau within the examined age range (56). While the gradual buildup of iron through midlife may be required for optimal brain function, the point where iron accumulation contributes to functional decline may mark the start of age-related cognitive loss (38). For example, in healthy older adults (65–79 years old), increased striatal iron levels correlated with lower scores on the dementia rating scale and longer reaction times on a two-choice attention test (107).

Similar to QSM findings in CUD (19), MFC values did not correlate with age in the CUD group in any ROI, suggesting a loss of the age-related gradual iron deposition within the GP and striatum seen in normal aging. Instead, several individuals with CUD in their 20s had elevated MFC values that are comparable to the MFC values of control individuals in their 40s. This observation is consistent with histology findings of young monkeys exposed to methamphetamine with significantly elevated GP iron levels comparable to GP iron levels in control monkeys double their age (16). Although duration of cocaine use was previously found to correlate with QSM in lieu of age (19), we were unable to replicate this finding with any of the self-reported cocaine use measures and there was no distinct use pattern unique to the younger cocaine users. Thus, other unexamined mechanisms may be involved, including inflammation and genetic influences (40–44,47,79,80). Nonetheless, whereas the accumulation of brain iron in normal aging

gradually reaches a level where excess iron may begin to impede brain function (38), individuals with CUD may reach detrimental iron levels earlier in life. Indeed, impaired cognitive functioning and psychomotor acuity are reported in individuals with CUD spanning all ages (99–101).

Strengths, Limitations, and Future Studies

Given that there is only one existing study of iron homeostasis in CUD (19), replication of findings is paramount. A strength of this study is that we were able to corroborate previous QSM findings using MFC imaging (52–54). As detailed in the introductory paragraphs, QSM and MFC provide different but complementary information about the variable characteristics of iron on the MRI signal. The key distinction between the methods (62,63) is the length scale of the iron-generated MFIs that they detect—microscopic (i.e., intravoxel) for MFC imaging and macroscopic (i.e., intervoxel) for QSM. Although both metrics have improved sensitivity and specificity compared with conventional relaxation rate methods (51), they remain techniques under development and are potentially affected by tissue properties other than iron (52,109). These nuances are demonstrated by the variable correlations that MFC, QSM, and the R2* relaxation rate metrics have in control individuals with putative postmortem iron concentrations in normal aging (Supplemental Figure S2).

Study limitations are noted. Despite the large effect size of our findings, the limited sample size may have reduced statistical power to replicate previous findings of lower RN iron in CUD and the correlation of GPe iron with duration of cocaine use (19). Variability in cocaine use recall as well as clinical differences between studies may also contribute to this discrepancy. Importantly, because the majority of the CUD cohort were regular nicotine smokers, our findings are not specific to cocaine but rather are likely generalizable to psychostimulants that alter dopamine transmission. Moreover, because 2 control individuals were taking medications that could alter iron absorption (i.e., omeprazole and meloxicam), their inclusion may have introduced medication confounds. However, any potential confounds were not driving the findings given that the original results were replicated when the two control individuals were excluded (Supplemental Table S3). The cross-sectional design of this study also prevents causal inferences about the age-related findings as related to elevated GPi iron in CUD. Lastly, by focusing only on brain iron, we cannot comment on systemic iron or inflammation status in our cohort.

In conclusion, our findings implicate dysregulation of brain iron homeostasis in CUD and support further examination of iron homeostasis in addiction. Future in vivo and postmortem studies assessing inflammation and ferroptosis markers (81,82) are needed to confirm whether neuroinflammation and neurodegeneration are present. To identify which iron regulatory signals are disrupted in CUD, studies assessing iron-related proteins and the genetic influences on iron status are also required (24,80). In addition, concurrent studies within the central nervous system and periphery are needed, particularly because mild peripheral iron deficiency has been detected in CUD (19); these studies are especially important for identifying appropriate iron-related therapeutic strategies (110–112). Lastly, longitudinal studies are needed to tease out whether dynamic changes in iron homeostasis occur during different stages of CUD. For example, examining individuals with variable levels of cocaine use over time could elucidate whether iron levels fluctuate in the striatum and GP relative to the degree of use, inflammation, and cognitive functioning. Although much more work is needed to fully understand the role of iron homeostasis in the persistence of CUD, our study and the few existing studies of iron homeostasis in addiction (12–19) are promising because they may represent a novel avenue of therapy research.

ACKNOWLEDGMENTS AND DISCLOSURES

Funding was provided by the Klingenstein Third Generation Foundation (to VA) and the Litwin Foundation (to JAH).

JHJ and JAH are inventors with patents related to MFC imaging that are owned by New York University and licensed to Siemens Healthcare. VA, CAH, CEM, and WHD report no biomedical financial interests or potential conflicts of interest.

ARTICLE INFORMATION

From the Department of Neuroscience (VA, CEM, JHJ, CAH, JAH), Department of Psychiatry and Behavioral Sciences (WHD, CAH), Department of Radiology and Radiological Science (JHJ, JAH), and Department of Neurology (JAH), Medical University of South Carolina, Charleston, South Carolina.

Address correspondence to Vitria Adisetiyo, Ph.D., Department of Neuroscience, Medical University of South Carolina, 173 Ashley Ave., MSC 510, Charleston, SC 29425; E-mail: adisetiy@musc.edu.

Received Jul 18, 2018; revised Oct 26, 2018; accepted Nov 15, 2018.

Supplementary material cited in this article is available online at https://doi.org/10.1016/j.bpsc.2018.11.006

REFERENCES

1. Gerlach KK, Dasgupta N, Schnoll SH, Henningfield JE (2014): Epidemiology of stimulant misuse and abuse: Implications for future epidemiologic and neuropharmacologic research. Neuropharmacology 87:91–96.
2. Koob GF, Volkow ND (2010): Neurocircuitry of addiction. Neuropsychopharmacology 35:217–238.
3. Substance Abuse and Mental Health Services Administration (2014): Results from the 2013 National Survey on Drug Use and Health: Summary of National Findings. NSDUH Series H-48 HHS Publication No. (SMA) 14-4863. Washington, DC: Department of Health and Human Services.
4. Ashok AH, Mizuno Y, Volkow ND, Howes OD (2017): Association of stimulant use with dopaminergic alterations in users of cocaine, amphetamine, or methamphetamine: A systematic review and meta-analysis. JAMA Psychiatry 74:511–519.
5. Ma L, Steinberg JL, Moeller FG, Johns SE, Narayana PA (2015): Effect of cocaine dependence on brain connections: Clinical implications. Expert Rev Neurother 15:1307–1319.
6. Bickel WK, Snider SE, Quisenberry AJ, Stein JS, Hanlon CA (2016): Competing neurobehavioral decision systems theory of cocaine addiction: From mechanisms to therapeutic opportunities. Prog Brain Res 223:269–293.
7. Dackis CA, O'Brien CP (2001): Cocaine dependence: A disease of the brain's reward centers. J Subst Abuse Treat 21:111–117.
8. Phillips KA, Epstein DH, Preston KL (2014): Psychostimulant addiction treatment. Neuropharmacology 87:150–160.
9. Czoty PW, Stoops WW, Rush CR (2016): Evaluation of the "pipeline" for development of medications for cocaine use disorder: A review of translational preclinical, human laboratory, and clinical trial research. Pharmacol Rev 68:533–562.
10. Belin D, Jonkman S, Dickinson A, Robbins TW, Everitt BJ (2009): Parallel and interactive learning processes within the basal ganglia:

Relevance for the understanding of addiction. Behav Brain Res 199:89–102.
11. Keeler JF, Pretsell DO, Robbins TW (2014): Functional implications of dopamine D1 vs. D2 receptors: A "prepare and select" model of the striatal direct vs. indirect pathways. Neuroscience 282:156–175.
12. Nelson C, Erikson K, Pinero DJ, Beard JL (1997): In vivo dopamine metabolism is altered in iron-deficient anemic rats. J Nutr 127: 2282–2288.
13. Erikson KM, Jones BC, Beard JL (2000): Iron deficiency alters dopamine transporter functioning in rat striatum. J Nutr 130: 2831–2837.
14. Erikson KM, Jones BC, Hess EJ, Zhang Q, Beard JL (2001): Iron deficiency decreases dopamine D1 and D2 receptors in rat brain. Pharmacol Biochem Behav 69:409–418.
15. Jones BC, Wheeler DS, Beard JL, Grigson PS (2002): Iron deficiency in rats decreases acquisition of and suppresses responding for cocaine. Pharmacol Biochem Behav 73:813–819.
16. Melega WP, Lacan G, Harvey DC, Way BM (2007): Methamphetamine increases basal ganglia iron to levels observed in aging. NeuroReport 18:1741–1745.
17. Jenney CB, Alexander DN, Jones BC, Unger EL, Grigson PS (2016): Preweaning iron deficiency increases non-contingent responding during cocaine self-administration in rats. Physiol Behav 167: 282–288.
18. Juhas M, Sun H, Brown MRG, MacKay MB, Mann KF, Sommer WH, *et al.* (2017): Deep grey matter iron accumulation in alcohol use disorder. NeuroImage 148:115–122.
19. Ersche KD, Acosta-Cabronero J, Jones PS, Ziauddeen H, van Swelm RP, Laarakkers CM, *et al.* (2017): Disrupted iron regulation in the brain and periphery in cocaine addiction. Transl Psychiatry 7:e1040.
20. Beard JL, Dawson H, Pinero DJ (1996): Iron metabolism: A comprehensive review. Nutr Rev 54:295–317.
21. Stohs SJ, Bagchi D (1995): Oxidative mechanisms in the toxicity of metal ions. Free Radic Biol Med 18:321–336.
22. Bresgen N, Eckl PM (2015): Oxidative stress and the homeodynamics of iron metabolism. Biomolecules 5:808–847.
23. Anderson GJ, Frazer DM (2017): Current understanding of iron homeostasis. Am J Clin Nutr 106:1559S–1566S.
24. Morris G, Berk M, Carvalho AF, Maes M, Walker AJ, Puri BK (2018): Why should neuroscientists worry about iron? The emerging role of ferroptosis in the pathophysiology of neuroprogressive diseases. Behav Brain Res 341:154–175.
25. Taylor EM, Crowe A, Morgan EH (1991): Transferrin and iron uptake by the brain: Effects of altered iron status. J Neurochem 57: 1584–1592.
26. Moos T, Rosengren Nielsen T, Skjorringe T, Morgan EH (2007): Iron trafficking inside the brain. J Neurochem 103:1730–1740.
27. Rouault TA, Zhang DL, Jeong SY (2009): Brain iron homeostasis, the choroid plexus, and localization of iron transport proteins. Metab Brain Dis 24:673–684.
28. Duck KA, Connor JR (2016): Iron uptake and transport across physiological barriers. Biometals 29:573–591.
29. Beard JL, Connor JR (2003): Iron status and neural functioning. Annu Rev Nutr 23:41–58.
30. Ramsey AJ, Hillas PJ, Fitzpatrick PF (1996): Characterization of the active site iron in tyrosine hydroxylase. Redox states of the iron. J Biol Chem 271:24395–24400.
31. Daubner SC, Le T, Wang S (2011): Tyrosine hydroxylase and regulation of dopamine synthesis. Arch Biochem Biophys 508:1–12.
32. Beard J (2003): Iron deficiency alters brain development and functioning. J Nutr 133:1468S–1472S.
33. Unger EL, Paul T, Murray-Kolb LE, Felt B, Jones BC, Beard JL (2007): Early iron deficiency alters sensorimotor development and brain monoamines in rats. J Nutr 137:118–124.
34. Lozoff B (2011): Early iron deficiency has brain and behavior effects consistent with dopaminergic dysfunction. J Nutr 141:740S–746S.
35. Earley CJ, Connor J, Garcia-Borreguero D, Jenner P, Winkelman J, Zee PC, *et al.* (2014): Altered brain iron homeostasis and dopaminergic function in restless legs syndrome (Willis-Ekbom disease). Sleep Med 15:1288–1301.
36. McCann JC, Ames BN (2007): An overview of evidence for a causal relation between iron deficiency during development and deficits in cognitive or behavioral function. Am J Clin Nutr 85:931–945.
37. Sidrak S, Yoong T, Woolfenden S (2014): Iron deficiency in children with global developmental delay and autism spectrum disorder. J Paediatr Child Health 50:356–361.
38. Zecca L, Youdim MB, Riederer P, Connor JR, Crichton RR (2004): Iron, brain ageing and neurodegenerative disorders. Nat Rev Neurosci 5:863–873.
39. Uranga RM, Salvador GA (2018): Unraveling the burden of iron in neurodegeneration: Intersections with amyloid beta peptide pathology. Oxid Med Cell Longev 2018:2850341.
40. Fox HC, D'Sa C, Kimmerling A, Siedlarz KM, Tuit KL, Stowe R, *et al.* (2012): Immune system inflammation in cocaine dependent individuals: Implications for medications development. Hum Psychopharmacol 27:156–166.
41. Kousik SM, Napier TC, Carvey PM (2012): The effects of psychostimulant drugs on blood brain barrier function and neuroinflammation. Front Pharmacol 3:121.
42. Clark KH, Wiley CA, Bradberry CW (2013): Psychostimulant abuse and neuroinflammation: Emerging evidence of their interconnection. Neurotox Res 23:174–188.
43. Urrutia P, Aguirre P, Esparza A, Tapia V, Mena NP, Arredondo M, *et al.* (2013): Inflammation alters the expression of DMT1, FPN1 and hepcidin, and it causes iron accumulation in central nervous system cells. J Neurochem 126:541–549.
44. Harricharan R, Abboussi O, Daniels WMU (2017): Addiction: A dysregulation of satiety and inflammatory processes. Prog Brain Res 235:65–91.
45. Brown KT, Levis SC, O'Neill CE, Northcutt AL, Fabisiak TJ, Watkins LR, *et al.* (2018): Innate immune signaling in the ventral tegmental area contributes to drug-primed reinstatement of cocaine seeking. Brain Behav Immun 67:130–138.
46. Sajja RK, Rahman S, Cucullo L (2016): Drugs of abuse and blood-brain barrier endothelial dysfunction: A focus on the role of oxidative stress. J Cereb Blood Flow Metab 36:539–554.
47. Bachi K, Mani V, Jeyachandran D, Fayad ZA, Goldstein RZ, Alia-Klein N (2017): Vascular disease in cocaine addiction. Atherosclerosis 262:154–162.
48. Adisetiyo V, Jensen JH, Tabesh A, Deardorff RL, Fieremans E, Di Martino A, *et al.* (2014): Multimodal MR imaging of brain iron in attention deficit hyperactivity disorder: A noninvasive biomarker that responds to psychostimulant treatment? Radiology 272: 524–532.
49. Everitt BJ, Robbins TW (2005): Neural systems of reinforcement for drug addiction: From actions to habits to compulsion. Nat Neurosci 8:1481–1489.
50. Grahn JA, Parkinson JA, Owen AM (2008): The cognitive functions of the caudate nucleus. Prog Neurobiol 86:141–155.
51. Dusek P, Dezortova M, Wuerfel J (2013): Imaging of iron. Int Rev Neurobiol 110:195–239.
52. Jensen JH, Chandra R, Ramani A, Lu H, Johnson G, Lee SP, *et al.* (2006): Magnetic field correlation imaging. Magn Reson Med 55:1350–1361.
53. Jensen JH, Szulc K, Hu C, Ramani A, Lu H, Xuan L, *et al.* (2009): Magnetic field correlation as a measure of iron-generated magnetic field inhomogeneities in the brain. Magn Reson Med 61: 481–485.
54. Jensen JH, Helpern JA (2014): Characterization of brain iron with magnetic field correlation imaging. Future Neurol 9:247–250.
55. Schenck JF, Zimmerman EA (2004): High-field magnetic resonance imaging of brain iron: Brth of a biomarker? NMR Biomed 17:433–445.
56. Hallgren B, Sourander P (1958): The effect of age on the non-haemin iron in the human brain. J Neurochem 3:41–51.
57. Connor JR, Menzies SL, St Martin SM, Mufson EJ (1990): Cellular distribution of transferrin, ferritin, and iron in normal and aged human brains. J Neurosci Res 27:595–611.

58. Morris CM, Candy JM, Oakley AE, Bloxham CA, Edwardson JA (1992): Histochemical distribution of non-haem iron in the human brain. Acta Anat (Basel) 144:235–257.
59. Quintana C, Bellefqih S, Laval JY, Guerquin-Kern JL, Wu TD, Avila J, *et al.* (2006): Study of the localization of iron, ferritin, and hemosiderin in Alzheimer's disease hippocampus by analytical microscopy at the subcellular level. J Struct Biol 153:42–54.
60. Brooks RA, Vymazal J, Goldfarb RB, Bulte JW, Aisen P (1998): Relaxometry and magnetometry of ferritin. Magn Reson Med 40: 227–235.
61. Allen PD, St Pierre TG, Chua-anusorn W, Strom V, Rao KV (2000): Low-frequency low-field magnetic susceptibility of ferritin and hemosiderin. Biochim Biophys Acta 1500:186–196.
62. Schweser F, Deistung A, Lehr BW, Reichenbach JR (2011): Quantitative imaging of intrinsic magnetic tissue properties using MRI signal phase: An approach to in vivo brain iron metabolism? NeuroImage 54:2789–2807.
63. Langkammer C, Schweser F, Krebs N, Deistung A, Goessler W, Scheurer E, *et al.* (2012): Quantitative susceptibility mapping (QSM) as a means to measure brain iron? A post mortem validation study. NeuroImage 62:1593–1599.
64. Adisetiyo V, Jensen JH, Ramani A, Tabesh A, Di Martino A, Fieremans E, *et al.* (2012): In vivo assessment of age-related brain iron differences by magnetic field correlation imaging. J Magn Reson Imaging 36:322–331.
65. Mink JW (1996): The basal ganglia: Focused selection and inhibition of competing motor programs. Prog Neurobiol 50:381–425.
66. American Psychiatric Association (2000): Diagnostic and Statistical Manual of Mental Disorders, 4th ed., text revision. Washington, DC: American Psychiatric Association.
67. Sheehan DV, Lecrubier Y, Sheehan KH, Amorim P, Janavs J, Weiller E, *et al.* (1998): The Mini-International Neuropsychiatric Interview (M.I.N.I.): The development and validation of a structured diagnostic psychiatric interview for DSM-IV and ICD-10. J Clin Psychiatry 59(suppl 20):22–33; quiz 34–57.
68. Heatherton TF, Kozlowski LT, Frecker RC, Fagerstrom KO (1991): The Fagerstrom Test for Nicotine Dependence: A revision of the Fagerstrom Tolerance Questionnaire. Br J Addict 86:1119–1127.
69. Ebbert JO, Patten CA, Schroeder DR (2006): The Fagerstrom Test for Nicotine Dependence–Smokeless Tobacco (FTND-ST). Addict Behav 31:1716–1721.
70. Beck AT, Steer RA, Brown GK (1996): Manual for the Beck Depression Inventory-II. San Antonio, TX: Psychological Corporation.
71. Saunders JB, Aasland OG, Babor TF, de la Fuente JR, Grant M (1993): Development of the Alcohol Use Disorders Identification Test (AUDIT): WHO Collaborative Project on Early Detection of Persons With Harmful Alcohol Consumption-II. Addiction 88:791–804.
72. Porter DA, Heidemann RM (2009): High resolution diffusion-weighted imaging using readout-segmented echo-planar imaging, parallel imaging and a two-dimensional navigator-based reacquisition. Magn Reson Med 62:468–475.
73. Kellner E, Dhital B, Kiselev VG, Reisert M (2016): Gibbs-ringing artifact removal based on local subvoxel-shifts. Magn Reson Med 76:1574–1581.
74. Volkow ND, Ding YS, Fowler JS, Wang GJ, Logan J, Gatley JS, *et al.* (1995): Is methylphenidate like cocaine? Studies on their pharmacokinetics and distribution in the human brain. Arch Gen Psychiatry 52:456–463.
75. Ardekani BA, Guckemus S, Bachman A, Hoptman MJ, Wojtaszek M, Nierenberg J (2005): Quantitative comparison of algorithms for inter-subject registration of 3D volumetric brain MRI scans. J Neurosci Methods 142:67–76.
76. Benjamini Y, Hochberg Y (1995): Controlling the false discovery rate: A practical and powerful approach to multiple testing. J R Stat Soc Series B Stat Methodol 57:289–300.
77. Little KY, Ramssen E, Welchko R, Volberg V, Roland CJ, Cassin B (2009): Decreased brain dopamine cell numbers in human cocaine users. Psychiatry Res 168:173–180.
78. Dietrich JB (2009): Alteration of blood-brain barrier function by methamphetamine and cocaine. Cell Tissue Res 336:385–392.
79. Schipper HM (2012): Neurodegeneration with brain iron accumulation—Clinical syndromes and neuroimaging. Biochim Biophys Acta 1822:350–360.
80. Andrews NC (2000): Iron homeostasis: Insights from genetics and animal models. Nat Rev Genet 1:208–217.
81. Dixon SJ, Lemberg KM, Lamprecht MR, Skouta R, Zaitsev EM, Gleason CE, *et al.* (2012): Ferroptosis: An iron-dependent form of nonapoptotic cell death. Cell 149:1060–1072.
82. Yang WS, Stockwell BR (2016): Ferroptosis: Death by lipid peroxidation. Trends Cell Biol 26:165–176.
83. De Domenico I, Vaughn MB, Li L, Bagley D, Musci G, Ward DM, *et al.* (2006): Ferroportin-mediated mobilization of ferritin iron precedes ferritin degradation by the proteasome. EMBO J 25:5396–5404.
84. Friedman A, Arosio P, Finazzi D, Koziorowski D, Galazka-Friedman J (2011): Ferritin as an important player in neurodegeneration. Parkinsonism Relat Disord 17:423–430.
85. Alquist CR, McGoey R, Bastian F, Newman W 3rd (2012): Bilateral globus pallidus lesions. J La State Med Soc 164:145–146.
86. Renard D, Brunel H, Gaillard N (2009): Bilateral haemorrhagic infarction of the globus pallidus after cocaine and alcohol intoxication. Acta Neurol Belg 109:159–161.
87. De Roock S, Hantson P, Laterre PF, Duprez T (2007): Extensive pallidal and white matter injury following cocaine overdose. Intensive Care Med 33:2030–2031.
88. Nair G, Evans A, Bear RE, Velakoulis D, Bittar RG (2014): The anteromedial GPi as a new target for deep brain stimulation in obsessive compulsive disorder. J Clin Neurosci 21:815–821.
89. Klavir O, Winter C, Joel D (2011): High but not low frequency stimulation of both the globus pallidus and the entopeduncular nucleus reduces "compulsive" lever-pressing in rats. Behav Brain Res 216:84–93.
90. Djodari-Irani A, Klein J, Banzhaf J, Joel D, Heinz A, Harnack D, *et al.* (2011): Activity modulation of the globus pallidus and the nucleus entopeduncularis affects compulsive checking in rats. Behav Brain Res 219:149–158.
91. Redgrave P, Prescott TJ, Gurney K (1999): The basal ganglia: A vertebrate solution to the selection problem? Neuroscience 89: 1009–1023.
92. Kreitzer AC, Berke JD (2011): Investigating striatal function through cell-type-specific manipulations. Neuroscience 198:19–26.
93. Kalivas PW, Volkow ND (2005): The neural basis of addiction: A pathology of motivation and choice. Am J Psychiatry 162:1403–1413.
94. Surmeier DJ, Ding J, Day M, Wang Z, Shen W (2007): D1 and D2 dopamine-receptor modulation of striatal glutamatergic signaling in striatal medium spiny neurons. Trends Neurosci 30:228–235.
95. Dreyer JK, Herrik KF, Berg RW, Hounsgaard JD (2010): Influence of phasic and tonic dopamine release on receptor activation. J Neurosci 30:14273–14283.
96. Cui G, Jun SB, Jin X, Pham MD, Vogel SS, Lovinger DM, *et al.* (2013): Concurrent activation of striatal direct and indirect pathways during action initiation. Nature 494:238–242.
97. Zapata A, Minney VL, Shippenberg TS (2010): Shift from goal-directed to habitual cocaine seeking after prolonged experience in rats. J Neurosci 30:15457–15463.
98. Escalona PR, Adair JC, Roberts BB, Graeber DA (1997): Obsessive compulsive disorder following bilateral globus pallidus infarction. Biol Psychiatry 42:410–412.
99. Spronk DB, van Wel JH, Ramaekers JG, Verkes RJ (2013): Characterizing the cognitive effects of cocaine: A comprehensive review. Neurosci Biobehav Rev 37:1838–1859.
100. Rogers RD, Robbins TW (2001): Investigating the neurocognitive deficits associated with chronic drug misuse. Curr Opin Neurobiol 11:250–257.
101. Beveridge TJ, Gill KE, Hanlon CA, Porrino LJ (2008): Parallel studies of cocaine-related neural and cognitive impairment in humans and monkeys. Philos Trans R Soc Lond B Biol Sci 363:3257–3266.

102. Goldberg JA, Bergman H (2011): Computational physiology of the neural networks of the primate globus pallidus: Function and dysfunction. Neuroscience 198:171–192.
103. Bilgic B, Pfefferbaum A, Rohlfing T, Sullivan EV, Adalsteinsson E (2012): MRI estimates of brain iron concentration in normal aging using quantitative susceptibility mapping. NeuroImage 59:2625–2635.
104. Kopani M, Kopaniova A, Caplovicova M, Maruscakova L, Sisovsky V, Jakubovsky J (2014): Iron and its relation to glycoconjugates in human globus pallidus. Bratisl Lek Listy 115:362–366.
105. Suchdev PS, Williams AM, Mei Z, Flores-Ayala R, Pasricha SR, Rogers LM, *et al.* (2017): Assessment of iron status in settings of inflammation: Challenges and potential approaches. Am J Clin Nutr 106:1626S–1633S.
106. Raz N, Rodrigue KM, Haacke EM (2007): Brain aging and its modifiers: Insights from in vivo neuromorphometry and susceptibility weighted imaging. Ann N Y Acad Sci 1097:84–93.
107. Sullivan EV, Adalsteinsson E, Rohlfing T, Pfefferbaum A (2009): Relevance of iron deposition in deep gray matter brain structures to cognitive and motor performance in healthy elderly men and women: Exploratory findings. Brain Imaging Behav 3:167–175.
108. Bartzokis G, Lu PH, Tingus K, Mendez MF, Richard A, Peters DG, *et al.* (2010): Lifespan trajectory of myelin integrity and maximum motor speed. Neurobiol Aging 31:1554–1562.
109. Yablonskiy DA, Sukstanskii AL (2017): Effects of biological tissue structural anisotropy and anisotropy of magnetic susceptibility on the gradient echo MRI signal phase: Theoretical background. NMR Biomed Apr;30(4).
110. Sripetchwandee J, Pipatpiboon N, Chattipakorn N, Chattipakorn S (2014): Combined therapy of iron chelator and antioxidant completely restores brain dysfunction induced by iron toxicity. PLoS One 9:e85115.
111. Sripetchwandee J, Wongjaikam S, Krintratun W, Chattipakorn N, Chattipakorn SC (2016): A combination of an iron chelator with an antioxidant effectively diminishes the dendritic loss, tau-hyperphosphorylation, amyloids-β accumulation and brain mitochondrial dynamic disruption in rats with chronic iron-overload. Neuroscience 332:191–202.
112. Wongjaikam S, Kumfu S, Khamseekaew J, Sripetchwandee J, Srichairatanakool S, Fucharoen S, *et al.* (2016): Combined iron chelator and antioxidant exerted greater efficacy on cardioprotection than monotherapy in iron-overloaded rats. PLoS One 11:e159414.